









Conservation of Energetic Pathways for Electroautotrophy in the Uncultivated Candidate Order *Tenderiales*

 Brian J. Eddie,^a  Lina J. Bird,^a Claus Pelikan,^b  Marc Musmann,^c  Clara Martínez-Pérez,^{c,d} Princess Pinamang,^e
 Anthony P. Malanoski,^f  Sarah M. Glaven^a

^aCenter for Bio/Molecular Science and Engineering, Naval Research Laboratory, Washington, DC, USA

^bSolgate GmbH, IST Park, Klosterneuburg, Austria

^cCentre for Microbiology and Environmental Systems Science, Division of Microbial Ecology, University of Vienna, Vienna, Austria

^dInstitute of Environmental Engineering, ETH Zurich, Zürich, Switzerland

^eDepartment of Biology, Prairie View Agricultural and Mechanical University, Prairie View, Texas, USA

^fMaterials Science and Technology Division, Naval Research Laboratory, Washington, DC, USA

ABSTRACT Electromicrobiology can be used to understand extracellular electron uptake in previously undescribed chemolithotrophs. Enrichment and characterization of the uncultivated electroautotroph “*Candidatus Tenderia electrophaga*” using electromicrobiology led to the designation of the order *Tenderiales*. Representative *Tenderiales* metagenome-assembled genomes (MAGs) have been identified in a number of environmental surveys, yet a comprehensive characterization of conserved genes for extracellular electron uptake has thus far not been conducted. Using comparative genomics, we identified conserved orthologous genes within the *Tenderiales* and nearest-neighbor orders important for extracellular electron uptake based on a previously proposed pathway from “*Ca. Tenderia electrophaga*.” The *Tenderiales* contained a conserved cluster we designated *uetABCDEFGHIJ*, which encodes proteins containing features that would enable transport of extracellular electrons to cytoplasmic membrane-bound energy-transducing complexes such as two conserved cytochrome *cbb*₃ oxidases. For example, UetJ is predicted to be an extracellular undecaheme *c*-type cytochrome that forms a heme wire. We also identified clusters of genes predicted to facilitate assembly and maturation of electron transport proteins, as well as cellular attachment to surfaces. Autotrophy among the *Tenderiales* is supported by the presence of carbon fixation and stress response pathways that could allow cellular growth by extracellular electron uptake. Key differences between the *Tenderiales* and other known neutrophilic iron oxidizers were revealed, including very few *Cyc2* genes in the *Tenderiales*. Our results reveal a possible conserved pathway for extracellular electron uptake and suggest that the *Tenderiales* have an ecological role in coupling metal or mineral redox chemistry and the carbon cycle in marine and brackish sediments.

IMPORTANCE Chemolithotrophic bacteria capable of extracellular electron uptake to drive energy metabolism and CO₂ fixation are known as electroautotrophs. The recently described order *Tenderiales* contains the uncultivated electroautotroph “*Ca. Tenderia electrophaga*.” The “*Ca. Tenderia electrophaga*” genome contains genes proposed to make up a previously undescribed extracellular electron uptake pathway. Here, we use comparative genomics to show that this pathway is well conserved among *Tenderiales* spp. recovered by metagenome-assembled genomes. This conservation extends to near neighbors of the *Tenderiales* but not to other well-studied chemolithotrophs, including iron and sulfur oxidizers, indicating that these genes may be useful markers of growth using insoluble extracellular electron donors. Our findings suggest that extracellular electron uptake and electroautotrophy may be pervasive among the *Tenderiales*, and the geographic locations from which metagenome-assembled genomes were recovered offer clues to their natural ecological niche.

Editor Katherine McMahon, University of Wisconsin-Madison

This is a work of the U.S. Government and is not subject to copyright protection in the United States. Foreign copyrights may apply.

Address correspondence to Brian J. Eddie, Brian.Eddie@nrl.navy.mil.

The authors declare no conflict of interest.

Received 5 May 2022

Accepted 10 August 2022

Published 7 September 2022

KEYWORDS *Tenderiales*, electroautotrophy, metagenome-assembled genomes

Chemolithotrophic bacteria contribute to key ecological processes such as metal cycling and carbon fixation, yet laboratory isolation and cultivation remain elusive, hindering our understanding of their distribution and physiology. Electromicrobiology, the study of the movement of electrons into and out of microbial cells by using electrochemistry, can be used to enrich and characterize chemolithotrophic bacteria capable of direct extracellular electron uptake. “*Candidatus Tenderia electrophaga*” was enriched on an electrode from seawater and is proposed to couple direct electron uptake with reduction of O₂ and CO₂ fixation for growth (1–3). Originally classified as a member of the *Chromatiales* by 16S rRNA gene (16S) sequence homology, “*Ca. Tenderia electrophaga*” was moved to its own order, within *Gammaproteobacteria*, based upon a more detailed protein sequence-based phylogeny (4, 5). However, the relatedness of the *Tenderiales* to each other, including conservation of electron transfer proteins, and with other chemolithotrophs has not been determined.

Members of the *Tenderiales* have been identified from a number of environments by metagenomic surveys, with several complete or nearly complete metagenome-assembled genomes (MAGs) being recovered from marine and estuarine sediments, hydrothermal vents, and floodplain sediments (4, 6, 7). Closely allied 16S sequences have been identified as probable sulfur-oxidizing symbionts of metazoans, although “*Ca. Tenderia electrophaga*” possesses only a limited suite of known sulfur oxidation enzymes (1). A proposed electron uptake pathway from “*Ca. Tenderia electrophaga*” has been described from genomics, transcriptomics, and proteomics data when grown on an electrode (2, 8), but the extent to which it is distributed across other bacterial species is unknown. The electron uptake and energetics pathways were identified in part based upon similarities to pathways described in iron-oxidizing *Zetaproteobacteria*, *Acidithiobacillales*, and *Gallionellales*, including the *Cyc2* protein, several multiheme cytochromes, and reverse electron transport (9–12). This link to iron oxidation is further supported by the experiments showing that a microbial community with “*Ca. Tenderia electrophaga*” as the primary electrotoph utilized electrodes as electron donors up to approximately 500 mV versus a standard hydrogen electrode, which is within the range expected for iron oxidation with O₂ as the electron acceptor (1, 13).

Given the emergence of publicly available metagenomic data sets that include putative *Tenderiales* spp., we used comparative genomics to further explore the distribution of putative electron transfer proteins from “*Ca. Tenderia electrophaga*.” We first determined the phylogenetic relationships within the *Tenderiales* order and to closely related orders and other bacteria capable of electron uptake. We then identified orthologous genes among these different groups and looked for those that were (i) previously identified as part of the “*Ca. Tenderia electrophaga*” electron uptake pathway, or (ii) encoded proteins with potential roles in electron transfer or electrode biofilms. We found several clusters of genes in addition to the previously noted undecaheme cluster that are likely involved in electron uptake, including a novel porin-cytochrome complex and associated cytochromes, orthologs of the cytochrome *cbb₃* oxidase complex, and a conserved hexaheme cytochrome. Comparison of the proposed electron uptake pathways from “*Ca. Tenderia electrophaga*” to more recently identified members of the *Tenderiales* and other chemolithotrophs offers potential biomarkers for their proposed biogeochemical role in oxidizing insoluble extracellular electron donors.

RESULTS

Phylogeny of the *Tenderiales*. A selection of 127 genomes and metagenome-assembled genomes (MAGs) (see Table S1 in the supplemental material) were used to establish the phylogenetic relationship among the *Tenderiales*, as well as between the *Tenderiales* and related orders or species suspected of chemolithoautotrophy via extracellular electron uptake. The *Tenderiales* in-group consisted of publicly available MAGs within the *Tenderiales* order defined by the Genome Taxonomy Database (GTDB) (4) and unpublished *Tenderiales* MAGs from magnetite-associated bacteria collected from beach sand at Juno and Omaha

beaches in Normandy, France (C. Martínez-Pérez, C. Pelikan, and M. Mußmann, unpublished data) (Table 1). Outgroup genomes and MAGs (here often referred to simply as genomes) were selected from the next closest orders in the GTDB taxonomy, from the NCBI *Chromatiales* taxonomy, and from known iron- and sulfur-oxidizing bacteria based upon prior observations that several genes found in “*Ca. Tenderia electrophaga*” have been implicated in iron or sulfur oxidation in other organisms (14).

“*Ca. Tenderia electrophaga*” NRL1 was the most complete MAG (99.63%) within the *Tenderiales* due to long-read sequencing from a highly enriched community. All other of the closed genome of strain NRL1 (3.66 Mbp).

A phylogenetic tree was constructed using an approximately 5,000-amino-acid alignment of conserved protein domains identified by the tool GTDB-tk (Fig. 1). This analysis placed all 16 of the *Tenderiales* into a single well-supported clade most closely related to the putative order SZUA-140 identified in the GTDB. This genomic comparison was complemented by a second phylogenetic tree constructed from the 31 nearly full-length *Tenderiales* 16S rRNA gene sequences (>1,350) in the ARB-Silva nonredundant database and 16S sequences extracted from the genomes and MAGs (Fig. S1), although it was not possible to determine the relationship between the *Tenderiales* and group 2 MAGs due to the lack of high-quality 16S rRNA genes identified in these MAGs.

Conserved genes within the *Tenderiales* MAGs. We assigned groupings to genomes used for phylogenetic comparison based on relatedness to the *Tenderiales* in order to describe the distribution of genes for extracellular electron uptake (Fig. 1). Group 1 consisted of the *Tenderiales*. Group 2 consisted of 20 genomes representing the neighboring orders within the GTDB Ga0077554, GCA-2400775, JAADHS01, SURF-13, SZUA-140, and VBWC01. Groups 3 and 4 consisted mostly of orders formerly classified within the *Chromatiales*, but recently split into *Thiohalomonadales*, *Nitrosococcales*, *Nitrococcales*, and *Chromatiales*, among others (4). Group 5 consisted primarily of other iron- and sulfur-oxidizing species and some additional MAGs recovered from Normandy, France. Orthologous genes, genes descended from a common ancestor via speciation event or horizontal transfer but not gene duplication (15), were identified using Proteinortho (Table S2) (16). A set of orthologous genes identified across genomes is referred to as an orthogroup. Conservation of orthogroups was quantified based upon relatedness to the *Tenderiales* clade in the protein tree (Fig. 1). Orthogroups were named using the representative protein identifier from “*Ca. Tenderia electrophaga*” if present (e.g., GenPept accession no. ALP54624.1), or the first protein identifier in the arbitrary genome input order if an ortholog was not present in “*Ca. Tenderia electrophaga*” (e.g., GenPept accession no. ACL71705.1) (Table S2). A core orthogroup genome was constructed using a 75% cutoff, based on a mean completeness of 77% within the *Tenderiales* MAGs, which resulted in 390 genes unique to the *Tenderiales* (group 1), 508 genes shared between the *Tenderiales* and group 2, and 366 genes common to groups 1 to 4 (Fig. S2).

Conserved proteins for extracellular electron uptake. While direct electron uptake has been noted for a range of microbial species (17), no universal conserved genetic markers for proteins involved in this process have been identified. “*Ca. Tenderia electrophaga*” has been proposed to take up electrons from electrodes via several multiheme cytochromes and other predicted periplasmic, outer membrane, and extracellular proteins (1). Therefore, we looked for genes and gene clusters (orthogroups with a conserved gene order) (Fig. 2) for these proteins across all five groups.

(i) Undecaheme cytochrome, triheme cytochrome domains, and NHL repeats. We previously noted that genes for an undecaheme and three triheme *c*-type cytochromes were collocated on the “*Ca. Tenderia electrophaga*” genome and were highly expressed during extracellular electron transfer (EET) regardless of electrode potential (2). These genes were part of a block of genes encoding 18 orthogroups (Table S4) that were highly conserved among the *Tenderiales* and group 2 organisms (Fig. 1, black squares). Furthermore, the order of genes was remarkably well conserved (Fig. 2A), indicating selective pressure for collocation. Here, we name the first 10 of these genes *uetABCDEFGHIJ*, for undecaheme electron transfer, and we refer to this region as the

TABLE 1 Genomes and MAGs used in this study

Bin ID	Name	CheckM completeness	Assembled length (bp)	number contigs	Environment	Reference or BioProject accession no.
GCA_011330695	" <i>Ca. Tenderia</i> sp."	70.69	2,657,668	659	Hydrothermal sediment	6
FCS_M_Gamma_047	MAG FCS_M_Gamma_047	94.36	4,775,750	250	Normandy magnetite	PRJEB54670
FCS_M_Gamma_048.1	" <i>Ca. Tenderia</i> electrophaga"	93.43	3,442,975	149	Normandy magnetite	PRJEB54670
3300032254_18	Not published metagenome bin	89.96	2,901,507	100	Damariscotta River Estuary (USA)	PRJNA539541
FO_M_Gamma_043.1	MAG FO_M_Gamma_043.1	85.59	3,075,132	243	Normandy magnetite	PRJEB54670
FCS_M_Gamma_047.1	MAG FCS_M_Gamma_047.1	84.28	3,032,772	134	Normandy magnetite	PRJEB54670
3300037424_47	Not published metagenome bin	85.6	2,906,281	319	Floodplain sediment, Riverton, Wyoming, USA	7
FO_M_Gamma_044	MAG FO_M_Gamma_044	80.47	2,414,050	463	Normandy magnetite	PRJEB54670
3300032260_22	Not published metagenome bin	86.71	2,396,328	216	Coastal sediment, Maine, USA	PRJNA539537
FO_M_Gamma_046.1	MAG FO_M_Gamma_046.1	74.52	2,486,236	246	Normandy magnetite	PRJEB54670
FCS_M_Gamma_048.2	MAG FCS_M_Gamma_048.2	64.99	1,816,566	88	Normandy magnetite	PRJEB54670
FO_M_Gamma_045	MAG FO_M_Gamma_045	56.73	2,313,911	624	Normandy magnetite	PRJEB54670
3300032373_40	Not published metagenome bin	50	2,221,472	280	Damariscotta River Estuary (USA)	PRJNA539537
GCA_011375055	" <i>Ca. Tenderia</i> sp."	37.93	1,287,708	460	Hydrothermal sediment (Pacific)	6
CP013099.1	" <i>Ca. Tenderia</i> electrophaga"	99.63	3,763,866	2	Marine sediment (Atlantic)	5
GCA_002415485	<i>Proteobacteria</i> bacterium UBA5122	92.33	2,962,318	88	Noosa River estuary sediment (Australia)	4

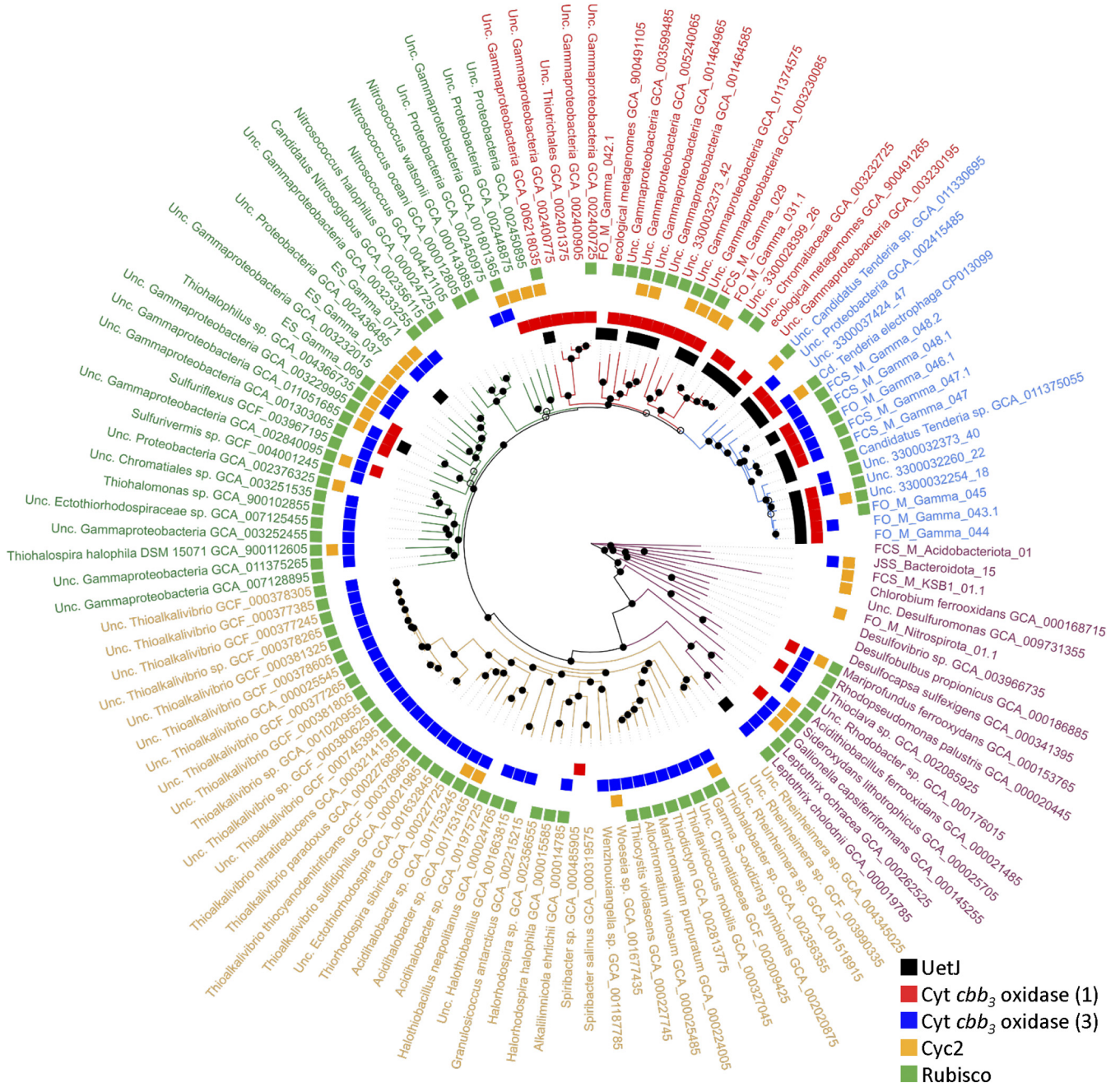


FIG 1 Phylogenetic tree constructed using an alignment of conserved proteins from metagenome bins and outgroup genomes identified by GTDB-tk. Group 1, *Tenderiales*, blue; group 2, GTDB neighboring orders, red ($n = 20$); group 3, GTDB next nearest neighboring orders, green ($n = 30$); group 4, *Chromatiales*, olive ($n = 43$); group 5, functional outgroup organisms, purple ($n = 18$). Taxonomic order names are from the GTDB. Open circles indicated bootstrap support of $>50\%$ for the node; filled circles indicate bootstrap support of $>75\%$. Colored boxes indicate presence of an ortholog for select marker proteins. For cytochrome *cbb₃* oxidase, the catalytic subunit CcoN was used for the marker protein, and for RuBisCO, presence of either a type I large subunit was used, or type II protein was used.

uet cluster, and we include the downstream conserved genes *ccsAB*, *nrfG*, and *batABD* as a conserved part of this module (Fig. 2).

The undecaheme protein UetJ (fig|666666.657277.peg.3443 encoded by Tel_16545), contained 11 CXXCH heme binding motifs but no other conserved functional domains. It is highly expressed (2), suggesting its designation as a pseudogene by NCBI is an annotation error. *In silico* structural predictions indicated a long bar shape with the heme binding domains lined up down the center of the protein less than 1 nm apart, which would allow for efficient electron transfer (18) (Fig. S3). It was predicted to contain a signal peptide for

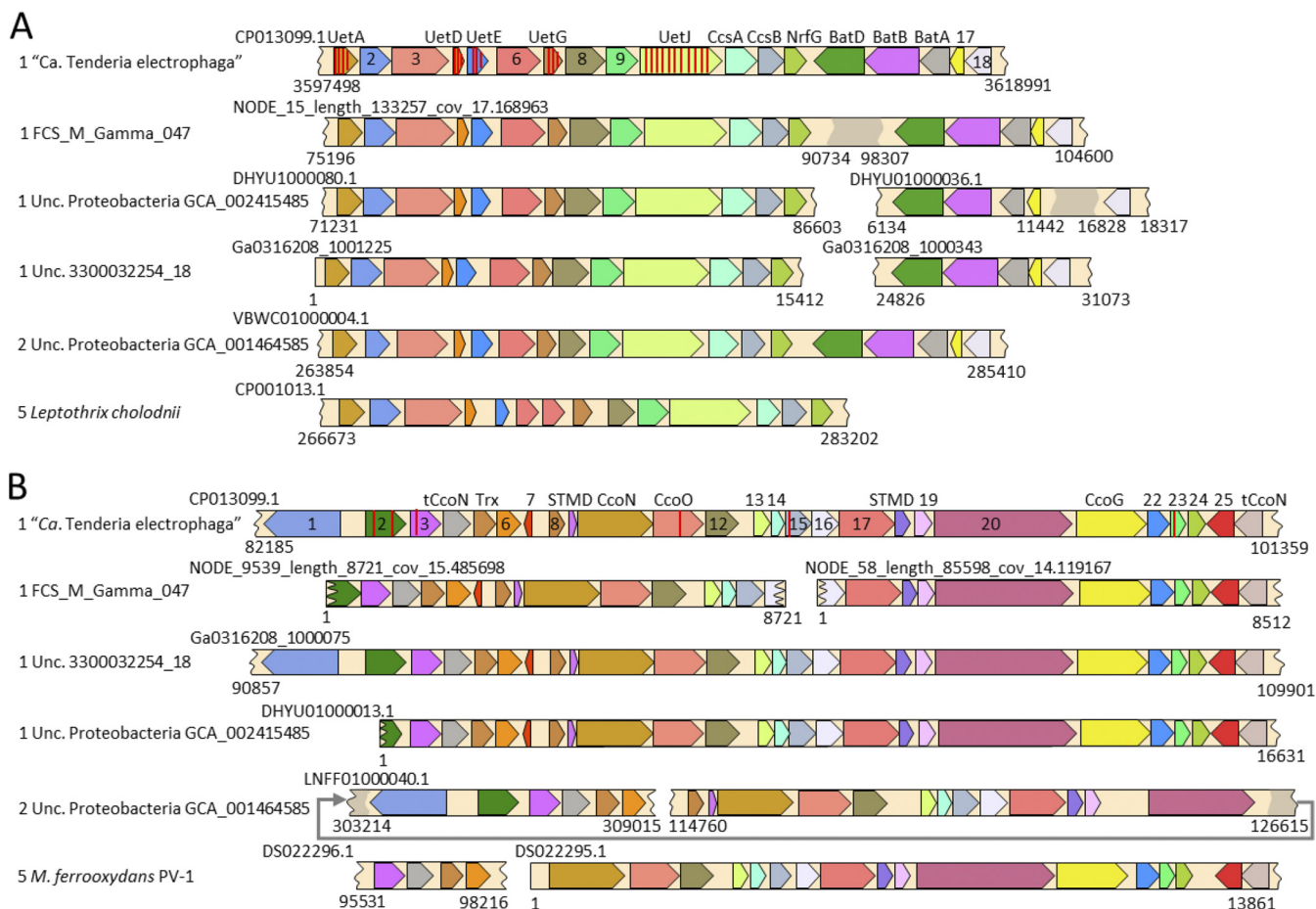


FIG 2 Synteny within conserved genes among the *Tenderiales*. (A) Gene order within the putative EET module found in the *Tenderiales* is highly conserved among a diverse selection of the *Tenderiales* and group 2 organisms, with an outlier found in *Leptothrix cholodnii*. Group number is shown before genome identifier. Orthologous genes share the same color, with labels shown for "Ca. Tenderia electrophaga" proteins. Heme binding domains are indicated with a red line. 2, GenPept accession no. [ALP54623.1](#), peptidylprolyl isomerase UetB; 3, GenPept accession no. [ALP54624.1](#), β -barrel outer membrane protein UetC; 6, GenPept accession no. [ALP54627.1](#), cupredoxin UetF; 8, GenPept accession no. [ALP54629.1](#) NHL repeat unit UetH; 9, GenPept accession no. [ALP54908.1](#), NHL repeat unit UetI; 17, GenPept accession no. [ALP54636.1](#), hypothetical protein; 18, GenPept accession no. [ALP54637.1](#), YeaD2 superfamily. (B) The region containing cytochrome *cbb*₃ oxidases 1 and 2 is conserved among the *Tenderiales* and some more distantly related organisms. 1, GenPept accession no. [ALP51721.1](#); 2, GenPept accession no. [ALP51722.1](#), diheme cytochrome; 3, GenPept accession no. [ALP51723.1](#), monoheme cytochrome; tCcoN, truncated CcoN protein; 6, GenPept accession no. [ALP51726.1](#); 7, GenPept accession no. [ALP51727.1](#); 8, GenPept accession no. [ALP51728.1](#); 12, GenPept accession no. [ALP51731.1](#); 13, GenPept accession no. [ALP51732.1](#); 14, GenPept accession no. [ALP51733.1](#); 15, GenPept accession no. [ALP51734.1](#), monoheme cytochrome; 16, GenPept accession no. [ALP51735.1](#); 17, GenPept accession no. [ALP51736.1](#), serine threonine protein kinase; 19, GenPept accession no. [ALP51738.1](#); 20, GenPept accession no. [ALP54674.1](#); 22, GenPept accession no. [ALP51740.1](#); 23, GenPept accession no. [ALP51741.1](#), monoheme cytochrome; 24, GenPept accession no. [ALP51742.1](#); 25, GenPept accession no. [ALP51743.1](#).

export from the cytoplasm and was predicted to be an extracellular protein by pSort3.0 (19). UetC (GenPept accession no. [ALP54624.0](#)) was a predicted β -barrel protein that could form a pore into which an electron transfer protein is inserted, much as MtrA fits inside MtrB (20). In contrast to MtrB, which contains 26 transmembrane strands, UetC was predicted by PRED-TMBB2 to contain 28 transmembrane strands, which likely gives it a larger pore size (21). This was borne out in the structural model, with a pore of approximately 5 nm diameter (Fig. S3).

UetDEG proteins (GenPept accession no. [ALP54625.1](#)/Tel_16515, GenPept accession no. [ALP54626.1](#)/Tel_16520, and GenPept accession no. [ALP54628.1](#)/Tel_16530) each contained a *c*₇-type triheme domain previously identified in periplasmic electron transfer proteins from *Geobacter sulfurreducens* (22). The best structurally characterized of the *G. sulfurreducens* proteins, the periplasmic dodecaheme *c*-type cytochrome GSU1996, contains four such triheme domains (A, B, C, and D) (22), of which all three "Ca. Tenderia electrophaga" orthologs best match domain C. UetF (GenPept accession no. [ALP54627.1](#)) contains a predicted cupredoxin domain, which has been associated with electron transfer

via a Cu^{+1} ion. Proteins with a single cupredoxin domain are often found as soluble electron carriers, such as azurin, rusticyanin, and plastocyanin. However, UetF was much larger than these proteins and may have a different role here.

UetH and UetI (GenPept accession nos. [ALP54629.1](#) and [ALP54908.1](#)) contained NHL domains and a β -propeller structure that is sometimes associated with protein-protein interactions (23). UetH was predicted by PSORTb to be cytoplasmic, with a seven-bladed β -propeller structure, while UetI was predicted to be noncytoplasmic, with a six-bladed β -propeller structure. An NHL repeat domain-containing protein (Gmet_0556) was identified as being important in extracellular iron reduction in *Geobacter metallireducens*, most likely due to cellular adhesion (24) and stabilization of outer membrane cytochrome complexes in *Desulfovibrio ferrophilus* IS5 (25).

(ii) Cytochrome c maturation and assembly. The predicted orthogroups represented by GenPept accession nos. [ALP54630.1](#) and [ALP54631.1](#) were similar to the type II cytochrome maturation system proteins CcsA and CcsB, not commonly found in *Gammaproteobacteria*. The orthogroup represented by [ALP54632.1](#) contained tetratricopeptide repeat (TPR) domains and a partial NrfG domain, which have been shown to facilitate the maturation of multiheme cytochromes (26). The presence of this system in addition to the type I cytochrome maturation system might indicate some unusual aspect of the *Tenderiales*. For example, it has been speculated that anammox bacteria use the type II system as a second maturation complex dedicated toward maturation of multiheme cytochromes within the anammoxosome organelle (27). There is also recent evidence for horizontal gene transfer of cytochrome maturation systems along with EET modules (28).

(iii) Adhesion and metal binding domains. The *uet* cluster was adjacent to conserved orthogroups that were homologs of the *Bacteroides* AeroTolerance (BatI) operon (Fig. 2A), which can play a role in adhesion. The orthogroup represented by GenPept accession no. [ALP54633.1](#) contained a BatD domain with a single transmembrane domain, allowing it to be anchored in the outer membrane. In the *batI* operon, *batD* was preceded by a gene for the von Willebrand adhesion factor domain and TPR protein-protein interaction domain containing lipoprotein BatB (GenPept accession no. [ALP54634.1](#)) and BatA von Willebrand factor domain protein (GenPept accession no. [ALP54635.1](#)) (29). The metal ion-dependent adhesion site (MIDAS) motif DXSXS was conserved in both proteins near the N terminus. Originally associated with biofilm formation and adhesion in the presence of Mg^{2+} , this domain is associated with anodic EET in the Gram-positive bacterium *Enterococcus faecalis* by moderating some interaction with extracellular iron (30). The *Tenderiales* also contained a second BatABD operon represented by GenPept accession nos. [ALP52718.1](#) to [ALP52720.1](#) that was similar to the one discussed above.

(iv) Secondary c-type cytochrome-containing cluster. The *batI* operon in the “*Ca. Tenderiales electrophaga*” genome was followed by a 10-gene type I cytochrome maturation pathway found in most of the genomes examined here, as well as a cluster of 9 orthogroups that were conserved in the *Tenderiales* and group 2 organisms, with only a few representatives found in groups 3 to 5. Three of these orthogroups may be involved in regulation, with conserved domains for periplasmic ligand binding sensor domains (GenPept accession nos. [ALP54649.1](#) and [ALP54650.1](#)) and a heme-containing cyclic di-GMP phosphodiesterase (GenPept accession no. [ALP54651.1](#)). This cluster of genes encodes several potential electron transfer proteins, including a thioredoxin (GenPept accession no. [ALP54648.1](#)) and four multiheme cytochromes. These cytochromes consist of one with a partial CcoP domain (GenPept accession no. [ALP54909.1](#)), a pentaheme (GenPept accession no. [ALP54653.1](#)), and two triheme cytochromes (GenPept accession nos. [ALP54654.1](#) and [ALP54655.1](#)). The cytochrome represented by GenPept accession no. [ALP54655.1](#) also contained a CccA domain from superfamily cl30289, which is implicated as a periplasmic electron shuttle in iron oxidation (31). There was also an NHL domain protein (GenPept accession no. [ALP54653.1](#)), which may play a role in structuring these proteins into a complex.

Other potential electron transfer proteins. (i) Hexaheme cytochrome *c*. A small cluster of three genes encoding proteins with *c*-type cytochrome heme binding motifs was well conserved among the *Tenderiales*. Monoheme (GenPept accession no. [ALP52411.1](#)), hexaheme (GenPept accession no. [ALP52412.1](#)), and diheme cytochromes (GenPept accession no. [ALP52413.1](#)) were identified in 14, 15, and 16 of the 16 *Tenderiales* genomes, respectively, but were only collocated with each other in 10 of the 16 genomes. The hexaheme protein was predicted to be localized to the periplasm. Despite the presence of six heme binding domains, it does not appear to be closely related to other characterized hexaheme cytochromes, such as OmcS from *Geobacter sulfurreducens* or TherJR_1122 from *Therminicola potens* (32, 33). The diheme cytochrome contains a signal peptide and was predicted to be extracytoplasmic by pSort3.0, but no further functional prediction was possible. The monoheme cytochrome was predicted to be localized to the cytoplasmic membrane, with four predicted transmembrane helices predicted by Phobius and a CXXCH heme binding motif that was predicted to be exposed to the periplasm.

(ii) *Cyc2*. *Cyc2* is a biochemically verified iron oxidase and is widespread throughout several iron oxidizer lineages (9, 10, 34). “*Ca. Tenderia electrophaga*” was proposed to be an iron-oxidizing bacterium based, in part, on the presence of a *Cyc2* (GenPept accession no. [ALP52279.1](#)) (1). This protein was found in an orthogroup of only seven genes. Only one other member of the *Tenderiales* had a member of this orthogroup. Manual BLAST searches revealed 5 more orthogroups with a total of 36 additional proteins, bringing the total to 43 proteins spread across 36 genomes (Fig. 1); however, only 3 *Tenderiales* total had a *Cyc2* (“*Ca. Tenderia*” sp. strain 3300032254_18 encodes two different proteins). Because so few *Cyc2* homologs were identified within the *Tenderiales* and closely related MAGs (Fig. 1), it may function in an auxiliary role in EET in the *Tenderiales*, allowing strains that contain the gene to access additional electron donors. The *cyc2* gene containing members of the *Tenderiales* were not monophyletic, suggesting that this gene was acquired multiple times.

Electron transport chain. (i) Electron transfer to the quinone pool: conservation of the ACIII and *bc*₁ complex. In our model, upon entry into the cell through UetJ and one of several electron transfer proteins in the periplasm, electrons must travel to the terminal electron acceptor, O₂, or via the intramembrane quinone pool to reduce NAD⁺ for CO₂ reduction (Fig. 3). The *Tenderiales* possessed two conserved entry points into the quinone pool for electrons from EET, the alternative complex III (ACIII) and cytochrome *bc*₁ complex. The individual genes for both complexes were present in 9 to 15 of the genomes out of 16 total, depending on the gene.

The ACIII was originally described in bacteria due to the absence of the *bc*₁ complex (14), so the presence of a full *bc*₁ complex in addition to the ACIII suggests that they may fill separate functional roles, such as forward and reverse electron transport. Such a configuration has been hypothesized to be important to extracellular electron transfer and iron oxidation (2, 35, 36). We found that although the gene order was not always conserved, the gene cluster representing the ACIII complex was found in 11 of the *Tenderiales* and most of the group 2 organisms and the microaerophilic iron oxidizers.

The genes for the *cyt-bc*₁ complex were also present in most of the *Tenderiales* (13 to 15 genomes), and the proteins for the Rieske Fe-S subunit and cytochrome *b* were identified as orthologs of proteins in the majority of the outgroup genomes. However, the cytochrome *c*₁ orthologs were split into two different orthogroups, with the *Tenderiales* and about half of the group 2 organisms possessing members of one orthogroup which was uncommon outside the *Tenderiales*. This protein was similar enough to characterized cytochrome *bc*₁ complex subunits that the Conserved Domain Database identified it as a member of COG2857 ubiquinol-cytochrome *c* reductase; however, a second larger orthogroup of cytochrome *c*₁ proteins was identified in members of groups 3, 4, and 5. This second orthogroup did not contain any representatives from group 1 or 2 genomes, and members of the two orthogroups were mutually exclusive within a genome.

Both the NADH ubiquinone oxidoreductase (NUOR)- and succinate dehydrogenase

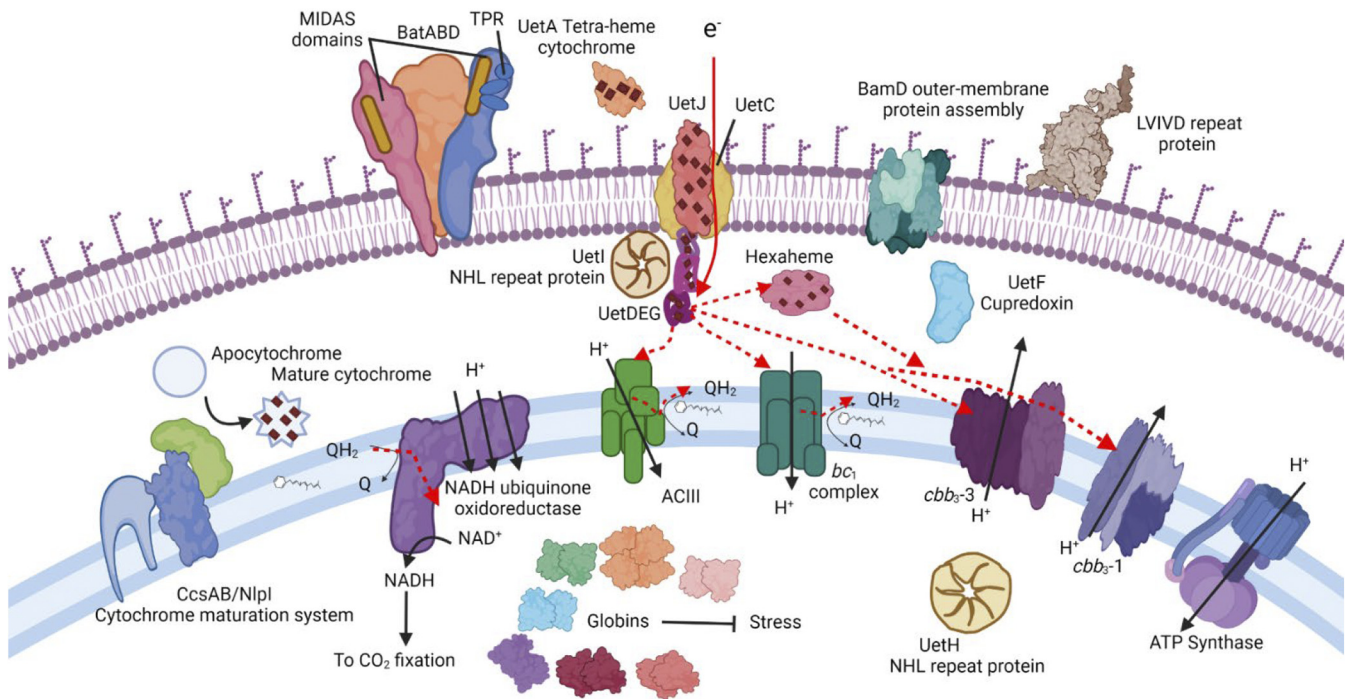


FIG 3 Predicted energetic pathway and auxiliary pathways found in the *Tenderiales*. The predicted electron flow in this model is shown with red arrows. Globins fulfill a stress response function. CcsAB/Nlp1 are proposed to be required for maturation of Uet cytochromes. The two BatABD complexes and the LVIVD repeat protein likely facilitate attachment to substrates. BamD and associated proteins are predicted to be required for maturation of outer membrane β -barrel proteins. Presence of individual pathway components in each MAG can be found in Table S2 in the supplemental material.

(SDH)-encoding regions were well conserved across all groups. NUOR is likely to be involved in reverse electron transport (2), accepting electrons from quinones and using proton motive force to reduce NAD^+ to NADH that can be used for anabolic processes within the cell as has been previously reported for a wide range of chemolithoautotrophs, including iron-oxidizing bacteria (35, 37). Indeed, 12 of the 16 *Tenderiales* MAGs, and most of the other genomes as well, encoded at least one form I RubisCO and the necessary anaplerotic enzymes for CO_2 fixation via the NADH-consuming Calvin-Benson-Bassham cycle (Table S4). SDH might allow heterotrophic growth based upon intracellular storage products, such as glycogen, or it might be used as a component of an incomplete tricarboxylic cycle to produce biosynthetic intermediates.

Terminal oxidases. We previously reported that “*Ca. Tenderia electrophaga*” encodes three cytochrome *cbb*₃ oxidase complexes, which are typically associated with microaerophilic respiration (2), and these complexes were conserved across the *Tenderiales*. The complex that was orthologous to the best studied representatives of *cbb*₃ oxidase consists of a full *cbb*₃-type cytochrome *c* oxidase (CcoNOQP; GenPept accession nos. ALP52999.1 to ALP53002.1). We predicted this to be the main terminal oxidase in the electron transport chain of “*Ca. Tenderia electrophaga*” on the basis of metatranscriptomics (2). It was present in most of the *Tenderiales* MAGs and was also common in other organisms. This region also encoded two conserved small single transmembrane domain (STMD) proteins that were rare outside the *Tenderiales* (fig|6666666.657277.peg.1551 and fig|6666666.657277.peg.1556). STMDs are small proteins (~35 amino acids [aa]) that have a single transmembrane domain with 5 to 10 exposed residues at either end. They are involved in assembly of respiratory complexes but have mostly been studied in a mitochondrial context (38). Genes encoding other *cbb*₃ accessory proteins were conserved within the *Tenderiales* as well, including FixHIS and the cytochrome *c* biogenesis protein DsbD. A gene encoding the ferredoxin FixG was only present in “*Ca. Tenderia electrophaga*” and two other members of the *Tenderiales* but was relatively common in groups 3, 4, and 5. This arrangement was also common in the endosymbiotic nitrogen-fixing bacteria, including *Ensifer meliloti*, which leads to an interesting possibility of horizontal gene transfer that is beyond the scope of this study (39).

A large region of 30 genes contained 26 orthogroups with a conserved arrangement (Fig. 2B) that were identified in most group 1 and 2 genomes and were nearly absent in groups 3 and 4. A similar arrangement of genes was identified in some freshwater iron-oxidizing bacteria (12), and in "*Ca. Tenderia electrophaga*" (2), with some of these genes representing the "distal" cytochrome *cbb*₃-oxidase identified by Ducluzeau et al. (40). Most predicted proteins in this region contain transmembrane helices or are membrane associated, suggesting that these proteins form a membrane-bound complex, with several proteins potentially facilitating assembly of the complex. The distal-*cbb*₃ type cytochrome *c* oxidase (GenPept accession nos. [ALP51729](#) and [ALP51730](#)) suggests this putative complex is likely involved in the electron transport chain and may generate proton motive force, a finding that is supported by recent work in *Sideroxydans lithotrophicus* ES-1 (41). The region also encodes two truncated CcoN proteins containing only 4 transmembrane helices each ([ALP51724.1](#) and [ALP51744.1](#)), 3 mono- and 1 diheme cytochromes, and 10 other proteins with one or more transmembrane domain (Table S4). Conservation of these genes within the *Tenderiales* and group 2 organisms suggests their function is also conserved. Their distribution was similar to the *uetA-J* genes, indicating a functional link between these two modules, but it is also possible this was an artifact of relatedness between the genomes because *cbb*₃ oxidase-1 and *cbb*₃ oxidase-3 were slightly more broadly distributed.

Other conserved regions of note. (i) Conserved globin proteins indicate stress response. We noted several conserved proteins related to stress response and biofilm formation, which are crucial processes for EET on electrodes. Seven proteins contained globin domains, which are associated with response to nitrite or oxygen stress (42). Referred to here as globin-1 through globin-7, they formed conserved orthogroups in *Tenderiales* but were rare in other groups (Table S4). Globin-1 (GenPept accession no. [ALP51974.1](#)) was found almost exclusively in *Tenderiales* and was adjacent to a 2-oxoglutarate-Fe(II) oxygenase (GenPept accession no. [ALP51975.1](#)), while globin-2 (GenPept accession no. [ALP52420.1](#)) is found in most *Tenderiales* and about half of their nearest neighbor orders. Some globins were also found in known iron-oxidizing bacteria, including the triple globin domain protein globin-3 (Ga0316208_100021114) in *Sideroxydans lithotrophicus* ES-1, globin-6 (GenPept accession no. [ALP54872.1](#)) in *Mariprofundus ferrooxidans* PV1, and globin-7 (Ga0316208_100045921) in *Rhodospseudomonas palustris* and *Acidithiobacillus ferrooxidans*. Globin-5 ([ALP54375.1](#)) was only conserved at 68.75%, but it was significantly more highly expressed under the more stressful condition in a biocathode metatranscriptome (2).

(ii) Uncharacterized surface and attachment proteins. The *Tenderiales* contained a number of unique, uncharacterized surface-associated proteins that may be important for biofilm formation on solid electron donors. These were identified by searching for domains involved in adhesion and screened for abundance ($\geq 75\%$) in the *Tenderiales* and rarity ($< 50\%$) in groups 3 and 4 (Table S3). Five orthogroups were found which contained adhesion-related histidine kinase or diguanylate cyclase domains. These could regulate attachment, as found in other electroactive biofilms (43, 44).

Several other orthogroups contained domains that suggested a role as extracellular structural components or secretion of exopolysaccharides. Thirteen *Tenderiales* had orthogroup [ALP52417.1](#), containing a bacterial polysaccharide deacetylase PgaB domain, required for export of biofilm-forming polysaccharides in *Staphylococcus epidermidis* (45). In five of the *Tenderiales*, this was paired with an orthogroup containing a PulE pilin secretion domain, which was not found in any other groups (GenPept accession no. [ALP52418.1](#)). The orthogroup represented by [ALP54212.1](#) was found only in the *Tenderiales* and contains an LVIVD repeat domain, which is associated with the cell surface of bacteria and archaea (46). This protein may form a β -propeller structure, which can be associated with protein-protein interactions (46). It was adjacent to the orthogroup represented by GenPept accession no. [ALP54213.1](#), which was also conserved in the *Tenderiales*, with no functional predictions. However, it does have a predicted signal peptide for export from the cytoplasm.

A cluster of four orthogroups that may export and assemble extracellular proteins

was mostly confined to the *Tenderiales*. The orthogroup represented by GenPept accession no. [ALP54158.1](#) had a BamD domain associated with folding and insertion of outer membrane β -barrel proteins (47), including the five TPR repeats required for protein function. This orthogroup was well conserved in the *Tenderiales* and less well conserved in the other groups here, with representation in 35% of group 2 organisms and 27% of group 3. It was followed by the orthogroup represented by GenPept accession no. [ALP54159](#), which contains three TPR repeats and was only found in the *Tenderiales* and two group 2 genomes, and GenPept accession no. [ALP54160.1](#), which was only found in the *Tenderiales* and did not have any conserved domains (48). The orthogroup represented by GenPept accession no. [ALP54162.1](#) was similar to the β -barrel protein BamA which is required for protein export (47) and was present in half of the *Tenderiales* genomes.

DISCUSSION

Here, comparative genomics was used to understand the metabolic potential of the *Tenderiales*. Based upon the conservation of genes for RubisCO and identification of genes that may be involved in EET, members of this order are likely all chemolithoautotrophs, using extracellular electron donors to fix CO₂. We described a key gene cluster, the *uet* cluster, conserved throughout the *Tenderiales* and several closely related orders, that encodes an extracellular undecaheme *c*-type cytochrome along with a number of other genes that likely play a role in EET and biofilm formation and maintenance. This *uet* cluster has not been implicated in EET in other bacterial lineages, but encoded proteins appear to follow the same structural rules identified in EET complexes, such as MtrCAB and PioAB, namely, an outer membrane β -barrel protein to provide a conduit into which multiheme cytochromes are inserted to transfer electrons across the outer membrane (49). This arrangement has previously been suggested to enable electron uptake from solid electron donors rather than only soluble electron donors as postulated for Cyc2 (34). While it is not possible to determine the precise role of each protein from bioinformatics methods alone, protein localization prediction tools suggest an extracellular location for the tetraheme cytochrome UetA and the undecaheme cytochrome UetJ and a periplasmic localization for the triheme cytochromes UetD, UetE, and UetG. All five of these proteins have predicted structures that place the hemes in a linear arrangement, ideal for transferring electrons over long distances. The predicted extracellular cytochromes UetJ and UetA may interact, with one acting as a transmembrane electron conduit. It is also possible that one or more of them forms long conductive polymers like those in *G. sulfurreducens* (33). This might enable electron transfer in the near-cell environment and may be responsible for the remarkable conductivity of a biocathode community containing “*Ca. Tenderia electrophaga*” (50).

Electrons entering the cell through such a pathway are then shuttled across the periplasm to the cytoplasmic membrane, where several options for energy conservation await. The *Tenderiales* contain several conserved modules that give them the ability to grow in a microaerophilic environment, such as two *cbb*₃-type terminal oxidases (51), indicating metabolic flexibility as seen in other organisms (52–54). Based on the previous metatranscriptomic results, the main terminal oxidase in the reduction of O₂ is most likely *cbb*₃ oxidase-3, but its role relative to the other terminal oxidase is unknown. The *Tenderiales* possess several electron transport chain components that are also found in iron-oxidizing bacteria, such as ACIII (55) and a cytochrome *bc*₁ complex with a unique *cyt-c*₁ protein that may indicate that it interacts with a unique redox partner, possibly for reverse electron transport. The presence of seven conserved globin genes in the *Tenderiales* may be a response to various oxidative or nitrosative stresses experienced by these organisms, similar to their proposed role in *Mariprofundus ferrooxydans* (12). The psychrophile *Pseudoalteromonas haloplanktis* contains four constitutively expressed globins that have been identified as playing distinct roles in reactive oxygen and nitrogen stress response (42, 56). The presence of a 2-oxoglutarate

Fe(II) oxygenase is intriguing because α -keto acids are known to have a peroxynitrite detoxifying effect, suggesting a connection between this globin orthogroup and nitrosative stress (57).

Biofilm formation is a key component of survival on an insoluble extracellular electron donor, and we see evidence for several unique orthogroups that may be involved in formation of biofilms. These range from BatABD proteins, which are similar to proteins that have been identified as critical for EET in *Streptococcus* (30), to polysaccharide secretion, which is necessary for forming the matrix of a biofilm. We also see a conserved orthogroup that is likely involved in assembly of outer membrane complexes, and an LVIVD domain protein, which may be involved in stabilizing interactions with extracellular proteins.

Microbial community surveys using the 16S rRNA gene and higher-resolution surveys using metagenomics have revealed the astonishing diversity of the bacterial world and allowed us to see that there is a considerable amount of diversity within the *Tenderiales*, including at least two major clades consisting of three genera. Several of the representative sequences were obtained from communities present on potential donors for EET, such as iron sulfide minerals (58), consistent with the prediction that they are capable of extracellular electron uptake. Most *Tenderiales* MAGs are from marine or brackish environments, but two were from river sediments (7), along with some of the *Tenderiales* 16S sequences (59). The most closely related MAGs were obtained from environments, including Normandy magnetite and hydrothermal vents, which might indicate a potential for an electroautotrophic lifestyle for these additional orders as well.

Furthermore, the high level of conservation of some predicted EET complexes and proteins within the *Tenderiales* and some of the most closely related orders suggests an important role for these components within cellular metabolism. We are not aware of any predicted metabolism for any members of the group 2 orders, but the presence of the *uetABCDEFGHJI* region in these MAGs suggests a shared function that we predict to be oxidation of extracellular electron donors. The closest cultivated strains to the *Tenderiales*, such as the *Nitrosococcales* and *Thiohalomonadales*, are chemolithoautotrophs, and the uncultivated organisms found in groups 1 and 2 also appear to be capable of chemolithoautotrophic growth, with RubisCO genes and potential EET conduits. All of this supports an ecological role for the *Tenderiales* in oxidizing insoluble electron donors such as iron minerals and fixing carbon within sediment.

The genes we have identified here expand our toolkit for beginning the process of engineering organisms that derive a biosynthetic advantage from using a bioelectrochemical system for redox balancing or supplemental energy to increase production efficiency (60–62). We have identified conserved protein-coding genes in the uncultivated order *Tenderiales*, including some which we propose form a novel conduit for EET. Control of the processes involved in the formation and maintenance of biofilms, as well as mitigation of stresses involved in this lifestyle, will be key to further development of these organisms for biotechnology.

MATERIALS AND METHODS

Selection and curation of genomes for analysis. Genome sequences, predicted protein sequences, and gene feature files for in-group and out-group genomes were downloaded in May of 2020 from NCBI (<https://www.ncbi.nlm.nih.gov>) if available. Genomes not available on NCBI were downloaded from the Integrated Microbial Genome database and updated in April of 2021 via release 202 of GTDB (63). Unpublished MAGs were annotated using RAST to generate the required files (64). The NCBI and RAST annotation pipelines mostly identified the same proteins, but to better standardize annotations between methods while retaining relevant NCBI identifiers for previously published genomes, all genomes were reannotated using the RAST pipeline, and the two annotations were merged. For proteins predicted by both methods, the original was retained. If reannotation predicted a protein where the original annotation predicted a pseudogene or no gene, the RAST annotation took precedence. Proteins identified by RAST have a gene identifier beginning with “fig.”

CheckM (65) was used to check genomes for completeness, contamination, and other general genome statistics (see Table S1 in the supplemental material). The tool GTDB-tk was used to identify genomes according to the GTDB taxonomy based upon conserved genes (Table S1) (66). Small subunit ribosomal RNAs (SSU

rRNAs) were identified within genomes and MAGs using the tool *ssu_finder*. Additional nonredundant, near-full-length (>1,350 bp) SSU-rRNA sequences for the *Tenderiales* were obtained from the Silva nonredundant (nr) database (67). This yielded 27 additional sequences.

Phylogenetic analysis of the *Tenderiales*. A protein-based phylogenetic reconstruction was created with conserved single-copy protein alignments obtained using CheckM. IQ-TREE (68) was used to reconstruct the phylogenetic tree using a maximum-likelihood algorithm with the Le and Gascuel model with frequencies and 10 rate categories (69). Confidence in branching order was assessed using 1,000 ultrafast approximate bootstraps. Phylogenetic trees were visualized using Iroki tree viewer (70). The protein-based phylogenetic tree was used to separate genomes into groups for further analysis.

Identification of conserved orthologous proteins. Orthologous predicted proteins were identified using Proteinortho v6.0.30 with the default settings (similarity, 95%; minimum identity, 25%; minimum coverage, 50%; synteny used; duplicates, 0; alpha, 0.5; purity, 1; minimum algebraic connectivity of orthologous groups during clustering, 0.1) and the PoFF extension. The default settings were highly conservative and resulted in splitting some clusters of proteins. Orthologous proteins that have been previously identified as being part of larger groups with different subtypes, i.e., RubisCO proteins and Cyc2 proteins, were identified by using BLAST to connect some of the initial clusters of orthologs that were more distantly related for final groupings reported in the paper (16). Conservation of orthogroups (15) was quantified for groups 1 to 5 defined above. We then identified the *Tenderiales* core genome consisting of genes for predicted proteins that are conserved in at least 75% of *Tenderiales* MAGs.

Synteny between genomes was visualized using SimpleSynteny (71) to identify protein-encoding genes that are conserved in order between genomes. The four *Tenderiales* MAGs selected for this were chosen based upon completeness and taxonomic coverage. For the putative electron transfer complex proteins, a MAG from a drinking water system metagenome (72) and the closed genome of the pure culture *Leptothrix cholodnii* (73) were chosen because they are more distantly related taxonomically, but contained the genes associated with this complex.

Additional publicly available bioinformatics tools were used for further characterization of conserved proteins (Table S4). Conserved domains were identified using the Conserved Domain Database hosted by the NCBI (74). Transmembrane helices were identified using Phobius (75). Outer membrane β -barrel predictions were performed using Pred-TMBB2 (21). Heme binding motifs were identified using the regular expression C.[2,4]CH in Notepad++ (<https://notepad-plus-plus.org/>). Homologous proteins that have been characterized in some way were identified using PaperBLAST (76). *In silico* structures were predicted using the Robetta webserver to run the RoseTTAFold deep learning tool (77). Predicted signal peptide sequences were removed prior to folding.

Data availability. Unpublished genome sequence data are available as BioProject accession no. PRJEB54670. Annotations used in this study are available on FigShare at https://figshare.com/articles/dataset/Data_for_Conservation_of_energetic_pathways_for_electroautotrophy_in_the_uncultivated_candidate_order_Tenderiales_/19632867.

SUPPLEMENTAL MATERIAL

Supplemental material is available online only.

FIG S1, TIF file, 1.1 MB.

FIG S2, TIF file, 0.1 MB.

FIG S3, TIF file, 1.8 MB.

TABLE S1, XLSX file, 0.03 MB.

TABLE S2, XLSX file, 17.3 MB.

TABLE S3, XLSX file, 1.7 MB.

TABLE S4, XLSX file, 0.02 MB.

ACKNOWLEDGMENTS

This work was funded through NRL's Base 6.1 program; the Office of Naval Research (ONR), N0001422WX00222 to S.M.G.; and the Austrian Science Fund (FWF), project ID P31010, awarded to M.M.

The opinions and assertions contained here are those of the authors and are not to be construed as those of the U.S. Navy, the military service at large, or the U.S. government.

REFERENCES

1. Wang Z, Leary DH, Malanoski AP, Li RW, Hervey WJ, Eddie BJ, Tender GS, Yanosky SG, Vora GJ, Tender LM, Lin B, Strycharz-Glaven SM. 2015. A previously uncharacterized, nonphotosynthetic member of the *Chromatiaceae* is the primary CO₂-fixing constituent in a self-regenerating biocathode. *Appl Environ Microbiol* 81:699–712. <https://doi.org/10.1128/AEM.02947-14>.
2. Eddie BJ, Wang Z, Hervey WJ, Leary DH, Malanoski AP, Tender LM, Lin B, Strycharz-Glaven SM. 2017. Metatranscriptomics supports the mechanism

- for biocathode electroautotrophy by “*Candidatus Tenderia electrophaga*.” *mSystems* 2:e00002-17. <https://doi.org/10.1128/mSystems.00002-17>.
3. Malanoski AP, Lin B, Eddie BJ, Wang Z, Hervey WJ, Glaven SM. 2018. Relative abundance of ‘*Candidatus Tenderia electrophaga*’ is linked to cathodic current in an aerobic biocathode community. *Microb Biotechnol* 11: 98–111. <https://doi.org/10.1111/1751-7915.12757>.
 4. Parks DH, Chuvochina M, Waite DW, Rinke C, Skarshewski A, Chaumeil P-A, Hugenholtz P. 2018. A standardized bacterial taxonomy based on genome phylogeny substantially revises the tree of life. *Nat Biotechnol* 36: 996–1004. <https://doi.org/10.1038/nbt.4229>.
 5. Eddie BJ, Wang Z, Malanoski AP, Hall RJ, Oh SD, Heiner C, Lin B, Strycharz-Glaven SM. 2016. ‘*Candidatus Tenderia electrophaga*’, an uncultivated electroautotroph from a biocathode enrichment. *Int J Syst Evol Microbiol* 66:2178–2185. <https://doi.org/10.1099/ijsem.0.001006>.
 6. Zhou Z, Liu Y, Xu W, Pan J, Luo Z-H, Li M. 2020. Genome-and community-level interaction insights into carbon utilization and element cycling functions of *Hydrothermarchaeota* in hydrothermal sediment. *mSystems* 5: e00795-19. <https://doi.org/10.1128/mSystems.00795-19>.
 7. Reji L, Cardarelli EL, Boye K, Bargar JR, Francis CA. 2022. Diverse ecophysiological adaptations of subsurface Thaumarchaeota in floodplain sediments revealed through genome-resolved metagenomics. *ISME J* 16: 1140–1152. <https://doi.org/10.1038/s41396-021-01167-7>.
 8. Leary DH, Hervey JW, Malanoski AP, Wang Z, Eddie BJ, Tender GS, Vora GJ, Tender LM, Lin B, Strycharz-Glaven SM. 2015. Metaproteomic evidence of changes in protein expression following a change in electrode potential in a robust biocathode microbiome. *Proteomics* 15:3486–3496. <https://doi.org/10.1002/pmic.201400585>.
 9. Castelle C, Guiral M, Malarte G, Ledgham F, Leroy G, Brugna M, Giudici-Ortoni M-T. 2008. A new iron-oxidizing/O₂-reducing supercomplex spanning both inner and outer membranes, isolated from the extreme acidophile *Acidithiobacillus ferrooxidans*. *J Biol Chem* 283:25803–25811. <https://doi.org/10.1074/jbc.M802496200>.
 10. McAllister SM, Polson SW, Butterfield DA, Glazer BT, Sylvan JB, Chan CS. 2020. Validating the Cyc2 neutrophilic iron oxidation pathway using meta-omics of *Zetaproteobacteria* iron mats at marine hydrothermal vents. *mSystems* 5: e00553-19. <https://doi.org/10.1128/mSystems.00553-19>.
 11. Appia-Ayme C, Guilian N, Ratouchniak J, Bonnefoy V. 1999. Characterization of an operon encoding two *c*-type cytochromes, an *aa3*-type cytochrome oxidase, and rusticyanin in *Thiobacillus ferrooxidans* ATCC 33020. *Appl Environ Microbiol* 65:4781–4787. <https://doi.org/10.1128/AEM.65.11.4781-4787.1999>.
 12. Emerson D, Field E, Chertkov O, Davenport K, Goodwin L, Munk C, Nolan M, Woyke T. 2013. Comparative genomics of freshwater Fe-oxidizing bacteria: implications for physiology, ecology, and systematics. *Front Microbiol* 4:254. <https://doi.org/10.3389/fmicb.2013.00254>.
 13. Bird LJ, Tender LM, Eddie B, Oh E, Phillips DA, Glaven SM. 2021. Microbial survival and growth on non-corrodible conductive materials. *Environ Microbiol* 23:7231–7244. <https://doi.org/10.1111/1462-2920.15810>.
 14. Pereira MM, Carita JN, Teixeira M. 1999. Membrane-bound electron transfer chain of the thermophilic bacterium *Rhodothermus marinus*: a novel multihemic cytochrome *bc*, a new complex III. *Biochemistry* 38: 1268–1275. <https://doi.org/10.1021/bi9818063>.
 15. Bronner G, Spataro B, Page M, Gautier C, Rechenmann F. 2002. Modeling comparative mapping using objects and associations. *Comput Chem* 26: 413–420. [https://doi.org/10.1016/s0097-8485\(02\)00004-9](https://doi.org/10.1016/s0097-8485(02)00004-9).
 16. Lechner M, Findeiss S, Steiner L, Marz M, Stadler PF, Prohaska SJ. 2011. Proteinortho: detection of (co-) orthologs in large-scale analysis. *BMC Bioinformatics* 12:124–129. <https://doi.org/10.1186/1471-2105-12-124>.
 17. Gupta D, Guzman MS, Bose A. 2020. Extracellular electron uptake by autotrophic microbes: physiological, ecological, and evolutionary implications. *J Ind Microbiol Biotechnol* 47:863–876. <https://doi.org/10.1007/s10295-020-02309-0>.
 18. Winkler JR, Gray HB. 2014. Long-range electron tunneling. *J Am Chem Soc* 136:2930–2939. <https://doi.org/10.1021/ja500215j>.
 19. Yu N, Wagner J, Laird M, Melli G, Rey S, Lo R, Dao P, Sahinalp S, Ester M, Foster L, Brinkman F. 2010. PSORTb 3.0: improved protein subcellular localization prediction with refined localization subcategories and predictive capabilities for all prokaryotes. *Bioinformatics* 26:1608–1615. <https://doi.org/10.1093/bioinformatics/btq249>.
 20. Edwards MJ, White GF, Butt JN, Richardson DJ, Clarke TA. 2020. The crystal structure of a biological insulated transmembrane molecular wire. *Cell* 181:665–673.e610. <https://doi.org/10.1016/j.cell.2020.03.032>.
 21. Tsigos KD, Elofsson A, Bagos PG. 2016. PRED-TMBB2: improved topology prediction and detection of beta-barrel outer membrane proteins. *Bioinformatics* 32:i665–i671. <https://doi.org/10.1093/bioinformatics/btw444>.
 22. Pokkuluri PR, Londer YY, Duke NEC, Pessanha M, Yang X, Orshonsky V, Orshonsky L, Erickson J, Zagayanskiy Y, Salgueiro CA, Schiffer M. 2011. Structure of a novel dodecaheme cytochrome *c* from *Geobacter sulfurreducens* reveals an extended 12 nm cytochrom with interacting hemes. *J Struct Biol* 174: 223–233. <https://doi.org/10.1016/j.jmb.2010.11.022>.
 23. Noegel AA, Rapp S, Lottspeich F, Schleicher M, Stewart M. 1989. The *Dictyostelium* gelation factor shares a putative actin binding site with alpha-actinins and dystrophin and also has a rod domain containing six 100-residue motifs that appear to have a cross-beta conformation. *J Cell Biol* 109:607–618. <https://doi.org/10.1083/jcb.109.2.607>.
 24. Smith JA, Lovley DR, Tremblay P-L. 2013. Outer cell surface components essential for Fe (III) oxide reduction by *Geobacter metallireducens*. *Appl Environ Microbiol* 79:901–907. <https://doi.org/10.1128/AEM.02954-12>.
 25. Deng X, Dohmae N, Nealsen KH, Hashimoto K, Okamoto A. 2018. Multiheme cytochromes provide a pathway for survival in energy-limited environments. *Sci Adv* 4:eaa05682. <https://doi.org/10.1126/sciadv.aao5682>.
 26. Han D, Kim K, Oh J, Park J, Kim Y. 2008. TPR domain of NrfG mediates complex formation between heme lyase and formate-dependent nitrite reductase in *Escherichia coli* O157: H7. *Proteins* 70:900–914. <https://doi.org/10.1002/prot.21597>.
 27. Frousi C, Speth DR, Reimann J, den Camp HJO, Allen JW, Keltjens JT, Jetten MS. 2013. Identification of the type II cytochrome *c* maturation pathway in anammox bacteria by comparative genomics. *BMC Microbiol* 13:265–268. <https://doi.org/10.1186/1471-2180-13-265>.
 28. Baker IR, Conley BE, Gralnick JA, Girguis PR. 2022. Evidence for horizontal and vertical transmission of Mtr-mediated extracellular electron transfer among the bacteria. *mBio* 13:e02904-21. <https://doi.org/10.1128/mbio.02904-21>.
 29. Tang YP, Dallas MM, Malamy MH. 1999. Characterization of the *BatI* (*Bacteroides* aerotolerance) operon in *Bacteroides fragilis*: isolation of a *B. fragilis* mutant with reduced aerotolerance and impaired growth in *in vivo* model systems. *Mol Microbiol* 32:139–149. <https://doi.org/10.1046/j.1365-2958.1999.01337.x>.
 30. Keogh D, Lam LN, Doyle LE, Matysik A, Pavagadhi S, Umashankar S, Low PM, Dale JL, Song Y, Ng SP, Boothroyd CB, Dunny GM, Swarup S, Williams RBH, Marsili E, Kline KA. 2018. Extracellular electron transfer powers *Enterococcus faecalis* biofilm metabolism. *mBio* 9:e00626-17. <https://doi.org/10.1128/mBio.00626-17>.
 31. Singer SW, Chan CS, Zemla A, VerBerkmoes NC, Hwang M, Hettich RL, Banfield JF, Thelen MP. 2008. Characterization of cytochrome 579, an unusual cytochrome isolated from an iron-oxidizing microbial community. *Appl Environ Microbiol* 74:4454–4462. <https://doi.org/10.1128/AEM.02799-07>.
 32. Carlson HK, Iavarone AT, Gorur A, Yeo BS, Tran R, Melnyk RA, Mathies RA, Auer M, Coates JD. 2012. Surface multiheme *c*-type cytochromes from *Thermincola potens* and implications for respiratory metal reduction by Gram-positive bacteria. *Proc Natl Acad Sci U S A* 109:1702–1707. <https://doi.org/10.1073/pnas.1112905109>.
 33. Wang F, Gu Y, O’Brien JP, Yi SM, Yalcin SE, Srikanth V, Shen C, Vu D, Ing NL, Hochbaum AI, Egelman EH, Malvankar NS. 2019. Structure of microbial nanowires reveals stacked hemes that transport electrons over micrometers. *Cell* 177:361–369.e310. <https://doi.org/10.1016/j.cell.2019.03.029>.
 34. Keffer JL, McAllister SM, Garber AI, Hallahan BJ, Sutherland MC, Rozovsky S, Chan CS. 2021. Iron oxidation by a fused cytochrome-porin common to diverse iron-oxidizing bacteria. *mBio* 12:e01074-21. <https://doi.org/10.1128/mBio.01074-21>.
 35. Barco RA, Emerson D, Sylvan JB, Orcutt BN, Meyers MEJ, Ramirez GA, Zhong JD, Edwards KJ. 2015. New insight into microbial iron oxidation as revealed by the proteomic profile of an obligate iron-oxidizing chemolithoautotroph. *Appl Environ Microbiol* 81:5927–5937. <https://doi.org/10.1128/AEM.01374-15>.
 36. Ishii T, Kawaiichi S, Nakagawa H, Hashimoto K, Nakamura R. 2015. From chemolithoautotrophs to electrolithoautotrophs: CO₂ fixation by Fe (II)-oxidizing bacteria coupled with direct uptake of electrons from solid electron sources. *Front Microbiol* 6:994. <https://doi.org/10.3389/fmicb.2015.00994>.
 37. Elbehti A, Brasseur G, Lemesle-Meunier D. 2000. First evidence for existence of an uphill electron transfer through the *bc1* and NADH-Q oxidoreductase complexes of the acidophilic obligate chemolithotrophic ferrous ion-oxidizing bacterium *Thiobacillus ferrooxidans*. *J Bacteriol* 182:3602–3606. <https://doi.org/10.1128/JB.182.12.3602-3606.2000>.
 38. Zickermann V, Angerer H, Ding MG, Nübel E, Brandt U. 2010. Small single transmembrane domain (STMD) proteins organize the hydrophobic subunits of large membrane protein complexes. *FEBS Lett* 584:2516–2525. <https://doi.org/10.1016/j.febslet.2010.04.021>.

39. Barnett MJ, Fisher RF, Jones T, Komp C, Abola AP, Barloy-Hubler F, Bowser L, Capela D, Galibert F, Gouzy J, Gurjal M, Hong A, Huizar L, Hyman RW, Kahn D, Kahn ML, Kalman S, Keating DH, Palm C, Peck MC, Surzycki R, Wells DH, Yeh KC, Davis RW, Federspiel NA, Long SR. 2001. Nucleotide sequence and predicted functions of the entire *Sinorhizobium meliloti* pSymA megaplasmid. *Proc Natl Acad Sci U S A* 98:9883–9888. <https://doi.org/10.1073/pnas.161294798>.
40. Ducluzeau A-L, Ouchane S, Nitschke W. 2008. The *cbb3* oxidases are an ancient innovation of the domain bacteria. *Mol Biol Evol* 25:1158–1166. <https://doi.org/10.1093/molbev/msn062>.
41. Zhou N, Keffer JL, Polson SW, Chan CS. 2022. Unraveling Fe (II)-oxidizing mechanisms in a facultative Fe (II) oxidizer, *Sideroxydans lithotrophicus* strain ES-1, via culturing, transcriptomics, and reverse transcription-quantitative PCR. *Appl Environ Microbiol* 88:e01595-21. <https://doi.org/10.1128/AEM.01595-21>.
42. Russo R, Giordano D, Riccio A, Di Prisco G, Verde C. 2010. Cold-adapted bacteria and the globin case study in the Antarctic bacterium *Pseudoalteromonas haloplanktis* TAC125. *Mar Genomics* 3:125–131. <https://doi.org/10.1016/j.margen.2010.09.001>.
43. Eddie BJ, Malanoski AP, Onderko EL, Phillips DA, Glaven SM. 2021. *Marinobacter atlanticus* electrode biofilms differentially regulate gene expression depending on electrode potential and lifestyle. *Biofilm* 3:100051. <https://doi.org/10.1016/j.biofilm.2021.100051>.
44. Koeksoy E, Bezuidt OM, Bayer T, Chan CS, Emerson D. 2021. Zetaproteobacteria pan-genome reveals candidate gene cluster for twisted stalk biosynthesis and export. *Front Microbiol* 12:679409. <https://doi.org/10.3389/fmicb.2021.679409>.
45. Itoh Y, Rice JD, Goller C, Pannuri A, Taylor J, Meisner J, Beveridge TJ, Preston JF, III, Romeo T. 2008. Roles of *pgaABCD* genes in synthesis, modification, and export of the *Escherichia coli* biofilm adhesin poly-beta-1,6-N-acetyl-D-glucosamine. *J Bacteriol* 190:3670–3680. <https://doi.org/10.1128/JB.01920-07>.
46. Adindla S, Inampudi KK, Guruprasad L. 2007. Cell surface proteins in archaeal and bacterial genomes comprising “LVIVD”, “RIVW” and “LGxL” tandem sequence repeats are predicted to fold as β -propeller. *Int J Biol Macromol* 41:454–468. <https://doi.org/10.1016/j.ijbiomac.2007.06.004>.
47. Albrecht R, Zeth K. 2011. Structural basis of outer membrane protein biogenesis in bacteria. *J Biol Chem* 286:27792–27803. <https://doi.org/10.1074/jbc.M111.238931>.
48. Blatch GL, Lässle M. 1999. The tetratricopeptide repeat: a structural motif mediating protein-protein interactions. *Bioessays* 21:932–939. [https://doi.org/10.1002/\(SICI\)1521-1878\(199911\)21:11<932::AID-BIES5>3.0.CO;2-N](https://doi.org/10.1002/(SICI)1521-1878(199911)21:11<932::AID-BIES5>3.0.CO;2-N).
49. He S, Barco RA, Emerson D, Roden EE. 2017. Comparative genomic analysis of neutrophilic iron(II) oxidizer genomes for candidate genes in extracellular electron transfer. *Front Microbiol* 8:1584. <https://doi.org/10.3389/fmicb.2017.01584>.
50. Yates MD, Eddie BJ, Kotloski NJ, Lebedev N, Malanoski AP, Lin BC, Strycharz-Glaven SM, Tender LM. 2016. Toward understanding long-distance extracellular electron transport in an electroautotrophic microbial community. *Energy Environ Sci* 9:3544–3558. <https://doi.org/10.1039/C6EE02106A>.
51. Pitcher RS, Watmough NJ. 2004. The bacterial cytochrome *cbb3* oxidases. *Biochim Biophys Acta* 1655:388–399. <https://doi.org/10.1016/j.bbapbio.2003.09.017>.
52. Jiménez Otero F, Chan CH, Bond DR. 2018. Identification of different putative outer membrane electron conduits necessary for Fe (III) citrate, Fe (III) oxide, Mn (IV) oxide, or electrode reduction by *Geobacter sulfurreducens*. *J Bacteriol* 200:e00347-18. <https://doi.org/10.1128/JB.00347-18>.
53. Zacharoff L, Chan CH, Bond DR. 2016. Reduction of low potential electron acceptors requires the CbCl inner membrane cytochrome of *Geobacter sulfurreducens*. *Bioelectrochemistry* 107:7–13. <https://doi.org/10.1016/j.bioelechem.2015.08.003>.
54. Jo J, Cortez KL, Cornell WC, Price-Whelan A, Dietrich LE. 2017. An orphan *cbb3*-type cytochrome oxidase subunit supports *Pseudomonas aeruginosa* biofilm growth and virulence. *Elife* 6:e30205. <https://doi.org/10.7554/eLife.30205>.
55. Kato S, Ohkuma M, Powell DH, Krepski ST, Oshima K, Hattori M, Shapiro N, Woyke T, Chan CS. 2015. Comparative genomic insights into ecophysiology of neutrophilic, microaerophilic iron oxidizing bacteria. *Front Microbiol* 6:1265. <https://doi.org/10.3389/fmicb.2015.01265>.
56. Coppola D, Giordano D, Milazzo L, Howes BD, Ascenzi P, di Prisco G, Smulevich G, Poole RK, Verde C. 2018. Coexistence of multiple globin genes conferring protection against nitrosative stress to the Antarctic bacterium *Pseudoalteromonas haloplanktis* TAC125. *Nitric Oxide* 73:39–51. <https://doi.org/10.1016/j.niox.2017.12.006>.
57. Varma SD, Hegde KR. 2007. Lens thiol depletion by peroxyinitrite. Protective effect of pyruvate. *Mol Cell Biochem* 298:199–204. <https://doi.org/10.1007/s11010-006-9352-y>.
58. Barco RA, Hoffman CL, Ramírez GA, Toner BM, Edwards KJ, Sylvan JB. 2017. In-situ incubation of iron-sulfur mineral reveals a diverse chemolithoautotrophic community and a new biogeochemical role for *Thiomicrospira*. *Environ Microbiol* 19:1322–1337. <https://doi.org/10.1111/1462-2920.13666>.
59. Bakermans C, Madsen EL. 2002. Diversity of 16S rDNA and naphthalene dioxygenase genes from coal-tar-waste-contaminated aquifer waters. *Microb Ecol* 44:95–106. <https://doi.org/10.1007/s00248-002-0005-8>.
60. Glaven SM. 2019. Bioelectrochemical systems and synthetic biology: more power, more products. *Microb Biotechnol* 12:819–823. <https://doi.org/10.1111/1751-7915.13456>.
61. Kracke F, Lai B, Yu S, Krömer JO. 2018. Balancing cellular redox metabolism in microbial electrosynthesis and electro fermentation, a chance for metabolic engineering. *Metab Eng* 45:109–120. <https://doi.org/10.1016/j.ymben.2017.12.003>.
62. TerAvest MA, Ajo-Franklin CM. 2016. Transforming exoelectrogens for biotechnology using synthetic biology. *Biotechnol Bioeng* 113:687–697. <https://doi.org/10.1002/bit.25723>.
63. Markowitz VM, Korzeniewski F, Palaniappan K, Szeto E, Werner G, Padki A, Zhao X, Dubchak I, Hugenholtz P, Anderson I, Lykidis A, Mavromatis K, Ivanova N, Kyrpidis NC. 2006. The integrated microbial genomes (IMG) system. *Nucleic Acids Res* 34:D344–D348. <https://doi.org/10.1093/nar/gkj024>.
64. Overbeek R, Olson R, Pusch GD, Olsen GJ, Davis JJ, Disz T, Edwards RA, Gerdes S, Parrello B, Shukla M, Vonstein V, Wattam AR, Xia F, Stevens R. 2014. The SEED and the Rapid Annotation of microbial genomes using Subsystems Technology (RAST). *Nucleic Acids Res* 42:D206–D214. <https://doi.org/10.1093/nar/gkt1226>.
65. Parks DH, Imelfort M, Skennerton CT, Hugenholtz P, Tyson GW. 2015. CheckM: assessing the quality of microbial genomes recovered from isolates, single cells, and metagenomes. *Genome Res* 25:1043–1055. <https://doi.org/10.1101/gr.186072.114>.
66. Chaumeil P-A, Mussig AJ, Hugenholtz P, Parks DH. 2019. GTDB-Tk: a toolkit to classify genomes with the Genome Taxonomy Database. *Bioinformatics* 36:1925–1927. <https://doi.org/10.1093/bioinformatics/btz848>.
67. Quast C, Pruesse E, Yilmaz P, Gerken J, Schweer T, Yarza P, Peplies J, Glöckner FO. 2013. The SILVA ribosomal RNA gene database project: improved data processing and web-based tools. *Nucleic Acids Res* 41:D590–D596. <https://doi.org/10.1093/nar/gks1219>.
68. Nguyen L-T, Schmidt HA, Von Haeseler A, Minh BQ. 2015. IQ-TREE: a fast and effective stochastic algorithm for estimating maximum-likelihood phylogenies. *Mol Biol Evol* 32:268–274. <https://doi.org/10.1093/molbev/msu300>.
69. Le SQ, Gascuel O. 2008. An improved general amino acid replacement matrix. *Mol Biol Evol* 25:1307–1320. <https://doi.org/10.1093/molbev/msn067>.
70. Moore RM, Harrison AO, McAllister SM, Polson SW, Wommack KE. 2020. Iroki: automatic customization and visualization of phylogenetic trees. *PeerJ* 8:e8584. <https://doi.org/10.7717/peerj.8584>.
71. Veltri D, Wight MM, Crouch JA. 2016. SimpleSynteny: a web-based tool for visualization of microsynteny across multiple species. *Nucleic Acids Res* 44:W41–W45. <https://doi.org/10.1093/nar/gkw330>.
72. Pinto AJ, Marcus DN, Ijaz UZ, Bautista-de Lose Santos QM, Dick GJ, Raskin L. 2016. Metagenomic evidence for the presence of comammox *Nitrospira*-like bacteria in a drinking water system. *mSphere* 1:e00054-15. <https://doi.org/10.1128/mSphere.00054-15>.
73. Emerson D, Ghiorse WC. 1992. Isolation, cultural maintenance, and taxonomy of a sheath-forming strain of *Leptothrix discophora* and characterization of manganese-oxidizing activity associated with the sheath. *Appl Environ Microbiol* 58:4001–4010. <https://doi.org/10.1128/aem.58.12.4001-4010.1992>.
74. Marchler-Bauer A, Lu SN, Anderson JB, Chitsaz F, Derbyshire MK, DeWeese-Scott C, Fong JH, Geer LY, Geer NC, Gonzales NR, Gwadz M, Hurwitz DI, Jackson JD, Ke ZX, Lanczycki CJ, Lu F, Marchler GH, Mullokandov M, Omelchenko MV, Robertson CL, Song JS, Thanki N, Yamashita RA, Zhang DC, Zhang NG, Zheng CJ, Bryant SH. 2011. CDD: a Conserved Domain Database for the functional annotation of proteins. *Nucleic Acids Res* 39:D225–D229. <https://doi.org/10.1093/nar/gkq1189>.
75. Käll L, Krogh A, Sonnhammer EL. 2007. Advantages of combined transmembrane topology and signal peptide prediction—the Phobius web server. *Nucleic Acids Res* 35:W429–W432. <https://doi.org/10.1093/nar/gkm256>.
76. Price MN, Arkin AP. 2017. PaperBLAST: text mining papers for information about homologs. *mSystems* 2:e00039-17. <https://doi.org/10.1128/mSystems.00039-17>.
77. Baek M, DiMaio F, Anishchenko I, Dauparas J, Ovchinnikov S, Lee GR, Wang J, Cong Q, Kinch LN, Schaeffer RD, Millán C, Park H, Adams C,

- Glassman CR, DeGiovanni A, Pereira JH, Rodrigues AV, van Dijk AA, Ebrecht AC, Opperman DJ, Sagmeister T, Buhlheller C, Pavkov-Keller T, Rathinaswamy MK, Dalwadi U, Yip CK, Burke JE, Garcia KC, Grishin NV, Adams PD, Read RJ, Baker D. 2021. Accurate prediction of protein structures and interactions using a three-track neural network. *Science* 373: 871–876. <https://doi.org/10.1126/science.abj8754>.
78. Pruesse E, Peplies J, Glöckner FO. 2012. SINA: accurate high-throughput multiple sequence alignment of ribosomal RNA genes. *Bioinformatics* 28:1823–1829. <https://doi.org/10.1093/bioinformatics/bts252>.
79. Kumar S, Stecher G, Li M, Knyaz C, Tamura K. 2018. MEGA X: molecular evolutionary genetics analysis across computing platforms. *Mol Biol Evol* 35:1547–1549. <https://doi.org/10.1093/molbev/msy096>.